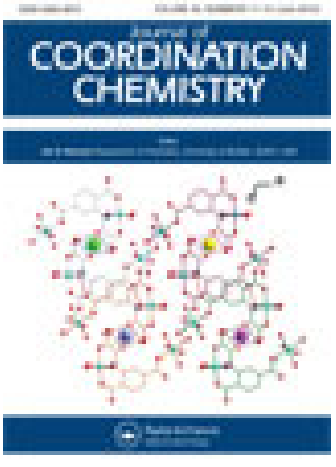

Journal of Coordination Chemistry
Publication details, including instructions for authors and subscription information:
http://www.tandfonline.com/loi/gcoo20

Phenolate-bridged zinc(II) complexes relevant to biological phosphoester cleavage

Katrin R. Grünwald [a], Manuel Volpe [a] & Nadia C. Mösch-Zanetti [a]
[a] Institute of Chemistry, Karl-Franzens-University Graz, Stremayrgasse 16, A-8010 Graz, Austria
Published online: 14 May 2012.

To cite this article: Katrin R. Grünwald, Manuel Volpe & Nadia C. Mösch-Zanetti (2012) Phenolate-bridged zinc(II) complexes relevant to biological phosphoester cleavage, Journal of Coordination Chemistry, 65:11, 2008-2020, DOI: 10.1080/00958972.2012.688117

To link to this article: http://dx.doi.org/10.1080/00958972.2012.688117

Journal of Coordination Chemistry
Vol. 65, No. 11, 10 June 2012, 2008–2020

Taylor & Francis
Taylor & Francis Group

Phenolate-bridged zinc(II) complexes relevant to biological phosphoester cleavage

KATRIN R. GRÜNWALD, MANUEL VOLPE
and NADIA C. MÖSCH-ZANETTI*

Institute of Chemistry, Karl-Franzens-University Graz, Stremayrgasse 16,
A-8010 Graz, Austria

(*Received 11 October 2011; in final form 2 April 2012*)

Three zinc complexes based on 2,6-bis(*N*-2-pyridylmethyl)formimidoyl-4-methylphenolate (**HL**) by employing $Zn(ClO_4)_2$, $Zn(CH_3COO)_2$, and $ZnCl_2$ have been synthesized and investigated as functional models of phosphoesterases. The molecular structure of $[\{Zn_2L(\mu^3\text{-}OH)(H_2O)\}_2](ClO_4)_4$ (**1**) obtained by reacting zinc perchlorate with **HL** was determined by X-ray diffraction analysis, revealing a tetranuclear species with four zinc centers and two ligands. Two zinc ions are accommodated within the two compartments of each ligand and are bridged by an additional hydroxide leading to Zn–Zn distances of 3.1235(9) and 3.1268(9) Å, respectively. The hydroxide is involved in an additional bridge to the second LZn_2 moiety forming a μ^3-OH. A water molecule is coordinated to two of the four zinc ions. The occurrence of a hydroxide group and of a coordinated water is relevant to the structure found in the native enzyme. The hydrolysis of the phosphoester bis(*p*-nitrophenol)phosphate ester (BNPP) in a mixture of DMSO and water at 50°C catalyzed by the three zinc compounds has been investigated. High hydrolytic activity was found for all three compounds but differed significantly depending on the nature of the counterion; the chloro derivative was found to be most active, while the perchlorate compound showed the least activity.

Keywords: Zinc; Phosphoester cleavage; Schiff base ligand

1. Introduction

Diphosphate esters are ubiquitous in nature, as they exhibit important functions in the transfer of information in DNA or RNA. According to their function, phosphatases can be divided into three classes [1]: monoesterases, such as purple acid phosphatase, cleave phosphate monoesters and play an important role in a number of human disorders, while diesterases hydrolyze DNA, RNA, or other phosphate diesters. Triphosphate esters are not known in nature, however some phosphatases are capable of hydrolyzing them; thus they can be utilized in the degradation of a number of pesticides or warfare agents.

The active sites of phosphatases are diverse in their structures. In general, enzymes capable of cleaving diphosphate esters accommodate two or more metal ions close to each other, mainly zinc, and also manganese, iron, or calcium are found in their active

*Corresponding author. Email: nadia.moesch@uni-graz.at

ISSN 0095-8972 print/ISSN 1029-0389 online
http://dx.doi.org/10.1080/00958972.2012.688117

sites [1–3]. A relevant structural feature of this class of enzymes is the distance between two metals in the active site, which seems to influence both the coordination mode of the phosphoester substrate and the mechanism of its cleavage. Accordingly, the substrate can bind to two metals in a η^2-O,O′ mode or to one metal only (η^1-O). For subsequent cleavage of the substrate, three main nucleophiles are proposed: a bridging hydroxide between the two metals, a terminal hydroxide, or an activated molecule of water on one metal [4]. In particular, in [Zn_2] enzymes the two cooperating zinc centers promote the cleavage of diphosphate esters [5, 6]: one of the two Lewis acidic metal centers activates a molecule of water forming a nucleophilic hydroxide ion, even at pH values below 8. The phosphate substrate coordinates to the other zinc center *via* one of the oxygen atoms, thereby increasing the electrophilicity of the phosphorus. The distance between the two metals given by the protein matrix, usually approximately 3.5 Å, brings the nucleophile and the substrate into optimal proximity for cleavage reactions. Specific functions of metals other than zinc are still a matter of discussion [2].

For a better understanding of mechanistic details of zinc containing phosphatases, small model complexes of the active site have been developed [7]. A common feature of the ligand architectures for such models is the presence of two compartments capable of accommodating a single zinc each, separated by various spacers. The nature of these linkers, either aliphatic or aromatic, determines the metal–metal distance that was found to crucially influence the effectiveness of such complexes in model cleavage reactions [8]. For example, the metal–metal separation of about 4 Å could be achieved by bridging N-containing aromatic heterocycles as shown by Meyer and coworkers [9, 10]. Depending on the length of the ancillary arms attached at the spacer, either Zn–(OH)–Zn or Zn–(OH)(H–OH)–Zn complex can be obtained. Other modeling approaches, leading to extremely high-cleavage activities, feature mononuclear [11, 12] and dinuclear [13] zinc complexes with ligands capable of intramolecular hydrogen bonding. Furthermore, phenolates with two adjacent donors were very versatile as the Zn–Zn separation is readily adjusted by the secondary bridging ligands (e.g., carboxylate, hydroxyl) [4, 14–26].

Herein, we present three dizinc complexes with a Schiff-base-derived phenolate ligand in which coordination to zinc occurs in two compartments of a planar O,N,N. The ligand has previously been used to coordinate copper ions, but no zinc complexes have as yet been prepared [27–30]. The activity of these zinc complexes was investigated toward the hydrolysis of bis(*p*-nitrophenol)phosphate ester (BNPP).

2. Experimental

2.1. *Materials and equipment*

2,6-bis(*N*-2-Pyridylmethyl)formimidoyl-4-methylphenolate (**HL**) was prepared according to a literature procedure [19]. All other chemicals were purchased from commercial sources and used without purification. All NMR spectra were measured on a Bruker Avance III spectrometer (300 MHz for ^{1}H). The ^{1}H NMR spectroscopic data are reported as s = singlet, d = doublet, t = triplet, m = multiplet or unresolved, br = broad signal, coupling constant(s) in Hz, shifts in ppm relative to the solvent residual peak. UV-Vis experiments were performed using a Varian Cary 50 spectrophotometer with a

thermally controlled cuvette holder. Infrared (IR) spectra were measured on a Bruker ALPHA–P Diamant ATR-FTIR spectrometer.

2.2. *Synthesis of 1–3*

Caution! Although no problems were encountered in this work, transition metal perchlorate complexes are potentially explosive and should be handled with proper precautions.

2.2.1. Synthesis of 1. To a boiling solution of **HL** (50 mg, 0.15 mmol) in ethanol (2 mL), solid zinc perchlorate hexahydrate (119 mg, 0.32 mmol) was added and boiling was maintained for an additional 30 min. The clear, yellow solution was allowed to cool to room temperature and was layered with diethyl ether to obtain a light yellow microcrystalline powder. The material was isolated by filtration, washed with diethyl ether, and dried under reduced pressure to yield 31 mg (34%) of $[\{Zn_2L(\mu^3\text{-}OH)(H_2O)\}_2](ClO_4)_4$ (**1**). Single crystals suitable for X-ray diffraction analysis were obtained by slow diffusion of diethyl ether into an ethanolic solution at −20°C. ^{1}H NMR (300 MHz, DMSO-d_6, 300 K): $\delta = 8.79$ (m, 4 H, $ArH_{Py} + N{=}CH$), 8.23 (t, $J = 7.5$ Hz, 2H, ArH_{Py}), 7.78 (m, 4H, ArH), 7.58 (s, 2H, ArH_{Ph}), 5.19 (s, 4H, N–CH_2), 4.17 (s, br, 2H, Zn–OH), 2.31 (s, 3H, Ph–CH_3), 2.22 (s, br, 1H, Zn–OH–Zn). IR (ATR, cm^{-1}): $\nu = 619$ (s), 762 (m), 1047 (s), 1542 (m), 1610 (s), 1637 (s), 3448 (br, H_2O). Anal. Calcd for $C_{42}H_{44}Cl_4N_8O_{22}Zn_4$ (%): C, 35.62; H, 3.13; N, 7.91. Found (%): C, 34.95; H, 3.26; N, 7.68.

2.2.2. Synthesis of 2. To a boiling solution of **HL** (50 mg, 0.15 mmol) in ethanol (2 mL), solid zinc acetate (59 mg, 0.32 mmol) was added and boiling was maintained for an additional 30 min after the reagent was dissolved. The clear, yellow solution was allowed to cool to room temperature and was layered with diethyl ether to obtain a yellow solid material, which was separated by centrifugation, washed with THF and diethyl ether, and dried under reduced pressure to yield 51 mg (52%) of $[Zn_2L(CH_3COO)_3]$ (**2**). ^{1}H NMR (300 MHz, DMSO-d_6, 300 K): $\delta = 8.73$ (s, 2H, N=CH), 8.62 (d, $J = 5.2$, 2H, ArH_{Py}), 8.12 (dt, $J = 7.7$, 1.4 Hz, 2H, ArH_{Py}), 7.66 (d, $J = 7.7$ Hz, 2H, ArH_{Py}), 7.61 (dt, $J = 7.7$, 1.4 Hz, 2H, ArH_{Py}), 7.55 (s, 2H, ArH_{Ph}), 5.16 (s, 4H, N–CH_2), 2.30 (s, 3H, Ph–CH_3), 1.82 (s, 9H, $3CH_3COO$). IR (ATR, cm^{-1}): $\nu = 642$ (m), 1020 (m), 1045 (m), 1410 (s, CO_2 symm str), 1559 (s, CO_2 asymm str), 2925 (w), 3300 (br, H_2O). Anal. Calcd for $C_{27}H_{28}N_4O_7Zn_2 \cdot 6H_2O$ (%): C, 42.70; H, 5.31; N, 7.38. Found (%): C, 43.74; H, 5.70; N, 7.41.

2.2.3. Synthesis of 3. To a boiling solution of **HL** (50 mg, 0.15 mmol) in *n*-butanol (2 mL), solid zinc chloride (44 mg, 0.32 mmol) was added. After a few seconds a voluminous yellow precipitate started to form and boiling was maintained for an additional 30 min. The suspension was allowed to cool to room temperature. The solid material was separated by centrifugation and was washed with THF and diethyl ether, and dried under reduced pressure to yield 80 mg (96%) of $[Zn_2LCl_3]$ (**3**). ^{1}H NMR (300 MHz, DMSO-d_6, 300 K): $\delta = 8.75$ (s, br, 4H), 7.94 (m, br, 2H), 7.62 (s, br, 4H), 7.47 (s, 2H), 5.11 (s, br, 4H, N–CH_2), 2.27 (s, 3H, Ph–CH_3). IR (ATR, cm^{-1}): $\nu = 767$ (s),

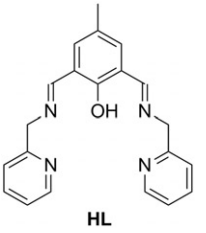

HL

Figure 1. Ligand **HL** used in this study.

1020 (m), 1046 (m), 1069 (m), 1287 (m), 1417 (s), 1540 (s), 1656 (s), 3488 (br, H_2O). Anal. Calcd for $C_{21}H_{19}Cl_3N_4O_1Zn_2 \cdot 2H_2O$ (%): C, 40.91; H, 3.76; N, 9.09. Found (%): C, 41.09; H, 3.57; N, 9.33.

2.3. *X-ray crystallographic studies*

The intensity data set for **1** was collected using a Bruker Smart Apex II diffractometer equipped with a graphite monochromator (Mo-Kα radiation, $\lambda = 0.71073$ Å) and a CCD detector and was measured at 100 K. The structure was solved by direct methods (SHELXS-97) and refined by full-matrix least-squares techniques against F^2 (SHELXL-97). All non-hydrogen atoms were refined with anisotropic displacement parameters without any constraints. Data were corrected for absorption and *L*p factors with SADABS [31]. Hydrogen atoms were placed geometrically and refined using a riding model, with the exception of hydroxyl protons (O3, O4) and water hydrogen atoms (O5, O6) that were found in the difference map. High-residual electron density ($+3.95$ e Å^{-3}) in the structure of **1** is located in close proximity of the already disordered perchlorate (Cl4C) and attempts to include it into the disorder modeling did not lead to any significant improvement.

3. Results and discussion

3.1. *Synthesis of 1–3*

HL (figure 1) is easily prepared in quantitative yield by the Schiff-base condensation of 2,6-diformyl-4-methylphenol and (2-aminomethyl)pyridine according to a literature procedure [19]. Only dicopper complexes have as yet been described, where two copper ions are accommodated in the two coordination pockets provided by the phenolate oxygen, the imine, and the pyridine nitrogen atoms with various secondary bridging ligands between two copper ions [27–30].

Dizinc complexes were prepared by reacting the ligand with three different zinc salts, as shown in scheme 1. Compound **1** was obtained by the treatment of a boiling solution of the ligand in ethanol with 2 equiv of $Zn(ClO_4)_2 \cdot 6H_2O$, leading to a deep yellow clear solution. After cooling to room temperature and layering with diethyl ether, a yellow material crystallized overnight at -20°C. X-ray diffraction analysis of a suitable single crystal revealed the formation of a tetranuclear 1 : 2 species (**1**) (vide infra).

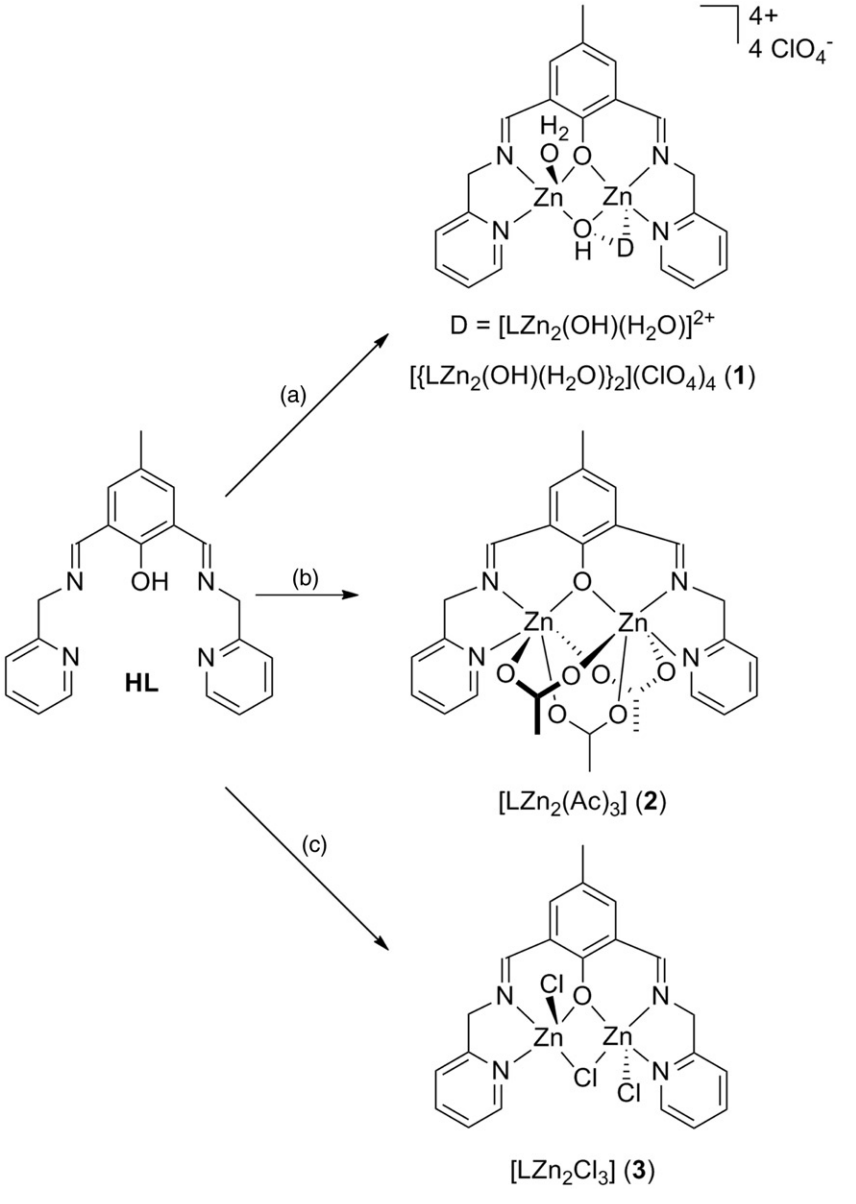

Scheme 1. Synthesis of **1**–**3**. (a) 2.2 eq. $Zn(ClO_4)_2 \cdot 6H_2O$, ethanol, 30 min reflux; (b) 2.2 eq. $Zn(CH_3COO)_2$, ethanol, 30 min reflux; (c) 2.2 eq. $ZnCl_2$, *n*-butanol, 20 min, 75°C (proposed structures in solution).

The compound is insoluble in THF or diethyl ether and is only moderately soluble in alcohols, acetonitrile, or chloroform. The solubility in DMSO is good enough for obtaining a ^{1}H NMR spectrum, but does not allow recording a ^{13}C NMR spectrum even with prolonged measurement. The ^{1}H NMR spectrum reveals a set of resonances assignable to the protons of a symmetrically coordinated ligand by showing only six signals in the aromatic region integrating for 12 protons with respect to the

methyl group. This fact indicates symmetric coordination of two metal ions with identical coordination patterns. However, according to the molecular structure determined by X-ray crystallography, the ligand environment is not symmetric, indicating dynamic behavior in solution. Low-temperature studies in order to slow down such a process were hampered by solubility issues.

A similar reaction procedure, as described above, employing $Zn(CH_3COO)_2$ results in a deep yellow clear solution. Complex **2** was isolated as a yellow precipitate after work up. The analogous reaction employing $ZnCl_2$ was performed in hot *n*-butanol, which led to the formation of a yellow voluminous precipitate for **3**. Both compounds display moderate solubility in alcohols, acetonitrile, or DMSO, but are insoluble in less polar solvents such as THF or ethers. The complexes are stable in the solid state, but decompose in solution at ambient conditions over several days. In ^{1}H NMR spectra of **2** and **3** signals for one ligand (shifted with respect to those of the free ligand) point to symmetric coordination of two zincs in both cases. Resonances of the CH_2 protons are a convenient tool to indicate the coordination. Whereas the chemical shift of these protons in the uncoordinated ligand appears at 4.90 ppm, they are shifted to 5.16 ppm in **2** and 5.11 ppm in **3**. In addition, the ^{1}H NMR spectrum of **2** shows a broad singlet at 1.82 ppm, which integrates for nine protons assignable to the methyls of three acetate counter ions. The broadness of the resonance is consistent with the observation that the pyridyl protons are poorly resolved in ^{1}H NMR spectra of **2** and **3**, indicating dynamic behavior in solution similar to **1**. Elemental analyses confirm the proposed complex stoichiometries.

3.2. *Molecular structure of 1*

Suitable single crystals for X-ray diffraction analysis of **1** were obtained by layering an ethanol solution with diethyl ether at −20°C. Molecular views are shown in figure 2, crystallographic data in table 1, and selected bond lengths and angles in table 2.

The structure analysis revealed a tetranuclear compound (**1**) with a metal to ligand ratio Zn : L = 2 : 1, consisting of two identical units $[Zn_2L(\mu\text{-OH})(H_2O)]^{2+}$ in which the two compartments of L are occupied by the two zinc ions. The hydroxide ion forms a bridge between both metals and one Zn is coordinated by water. The pre-organized binding pockets of the ligand are composed of the bridging phenolate O, the imine N, and the pyridine N. Each zinc is coordinated by L in an almost planar O,N,N fashion and by the bridging hydroxide. These four donors form the base of a distorted square pyramidal coordination sphere. The apical position at Zn1 is filled by a water molecule and at Zn2 by the hydroxide of the other unit. Thus, each zinc exhibits nearly ideal five-coordinate square pyramidal coordination with a N_2O_3 ligand sphere (structural index $\tau = 0.04$ (Zn1), 0.00 (Zn2), 0.26 (Zn3), and 0.02 (Zn4) [32]. The hydroxides are μ^3-OH bridging and form a tetranuclear species. The structure is complemented by four Cl_4O^- counterions. The hydrogen atoms on water could be located crystallographically as they are involved in hydrogen bonds to perchlorate. The μ^3-OH hydrogen on O3 and O4 were added completing a tetrahedral geometry typical for this type of oxygen.

The two identical units are twisted by an angle $\varphi = 87.8°$, φ being the angle between the ligand axes C14–O1 and C35–O2. The ligand planes ϵ_1 (defined as the least-square plane passing through C7–C15, N2 and N3) and ϵ_2 (C28–C36, N6 and N7) are not parallel between themselves, but form an angle of 10.2°. The pyridyl rings of the ligand

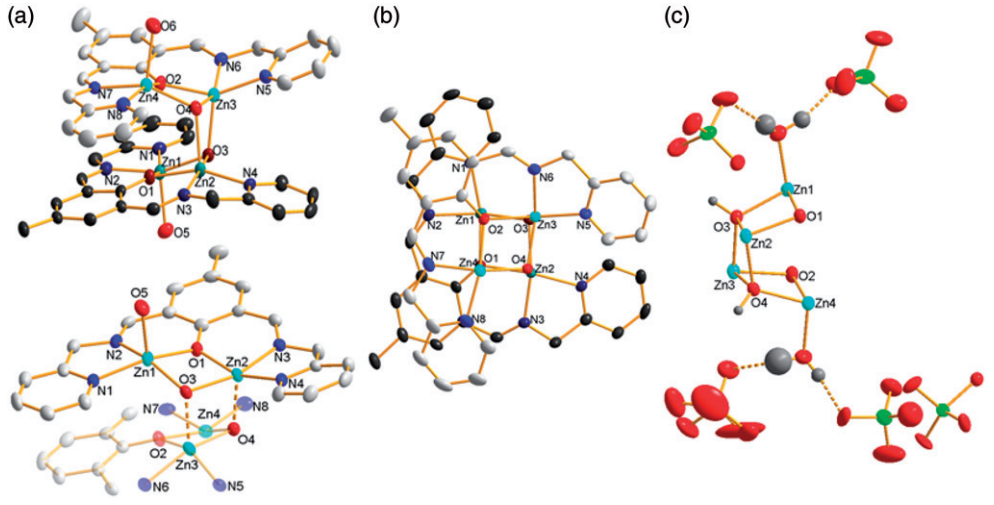

Figure 2. (a) Molecular structure of **1** (50% probability) and coordination mode at **HL**; (b) top view, bottom ligand depicted darker; (c) hetero-cubane structure of the Zn_4 core and hydrogen-bonding system of the coordinated water to the counter ions. Hydrogen atoms, coordinated water, and counter ions have been omitted for clarity where applicable.

Table 1. Crystallographic data and structure refinement for **1**.

	1
Empirical formula	$C_{42}H_{44}Cl_4N_8O_{22}Zn_4$
Formula weight	1416.13
Temperature (K)	100(2)
Crystal system	Monoclinic
Space group	$P2_1/c$
Unit cell dimensions (Å, °)	
a	10.8420(5)
b	13.2639(6)
c	37.1899(15)
α	90.00
β	92.072(2)
γ	90.00
Volume (Å^3), Z	5344.7(4), 4
Absorption coefficient (mm^{-1})	2.061
Reflections collected	46,971
Independent reflections	13,636 [R(int) = 0.0362]
Reflections with $I \geq 2\sigma(I)$	10,755
Goodness-of-fit on F^2	1.119
Final R indices [$I > 2\sigma(I)$]	$R_1 = 0.0701$, $wR_2 = 0.1724$
R indices (all data)	$R_1 = 0.0897$, $wR_2 = 0.1825$
Largest difference peak and hole (e Å^{-3})	3.955 and −0.704

accommodating Zn1 and Zn2 are twisted by 3.1° and 18.4° with respect to ϵ_1. The centroids of the pyridyl rings containing N1 and N4 deviate from ideal positions in the plane ϵ_1 by +0.24 Å and +0.71 Å, respectively. The planes of the pyridyl rings in the other ligand, which coordinates Zn3 and Zn4, are inclined by 9.7° and 22.5° with respect to ϵ_2. The centroids of these pyridyl rings containing N5 and N8 were located 1.06 and 0.53 Å above ϵ_2, respectively.

Table 2. Selected bond lengths (Å) and angles (°) for **1**.

Zn1–O1	2.055(4)	O1–Zn1–N1	159.04(17)
Zn1–N1	2.083(5)	O1–Zn1–N2	87.05(17)
Zn1–N2	2.049(5)	O1–Zn1–O3	80.93(15)
Zn1–O3	2.032(4)	O1–Zn1–O5	103.28(17)
Zn1–O5	2.049(4)	O1–Zn2–N3	88.54(17)
Zn2–O1	2.052(4)	O1–Zn2–N4	159.11(17)
Zn2–N3	2.032(5)	O1–Zn2–O4	95.05(16)
Zn2–N4	2.078(5)	O2–Zn3–N5	151.57(18)
Zn2–O3	2.083(4)	O2–Zn3–N6	86.86(18)
Zn2–O4	2.066(4)	O2–Zn3–O3	93.78(16)
Zn3–O2	2.056(4)	O2–Zn3–O4	79.10(16)
Zn3–N5	2.077(5)	O2–Zn4–N7	86.94(18)
Zn3–N6	2.037(5)	O2–Zn4–N8	159.53(19)
Zn3–O3	2.043(4)	O2–Zn4–O4	80.12(15)
Zn3–O4	2.073(4)	O2–Zn4–O6	96.4(2)
Zn4–O2	2.061(4)	O3–Zn2–O4	83.94(15)
Zn4–N7	2.041(5)	O3–Zn3–O4	84.76(15)
Zn4–N8	2.079(5)		
Zn4–O4	2.024(4)		
Zn4–O6	2.022(5)		
Zn1–Zn2	3.1235(9)		
Zn2–Zn3	3.0385(9)		
Zn3–Zn4	3.1268(9)		

The key motif of the structure is represented by an open Zn_4O_4 hetero-cubane core whose distortion is evidenced by the angles of the faces, which deviate from ideal geometry being between 80.12(15)° (for O2–Zn4–O4) and 95.05(16)° (for O1–Zn2–O4). The metal–metal distances of the two zincs that are found in one ligand are 3.1235(9) Å and 3.1268(9) Å for Zn1–Zn2 and Zn3–Zn4, respectively. The other Zn–Zn distances are 3.0385(9) Å for Zn2–Zn3 and 4.105(1) Å for Zn1···Zn4, consistent with an open face hetero-cubane structure. These Zn–Zn distances are similar to previously reported values for phenolate–dizinc–hydroxy fragments (3.16–3.02 Å) [25, 33], but are significantly shorter than in hydroxyl-bridged dizinc pyrazolate complexes (3.48 Å) [10] or acetate-bridged phenolate complexes (3.50–3.40 Å) [4, 18]. The two Zn–$O_{phenolate}$ bond lengths are essentially equivalent (2.052(4) Å for Zn2–O1 to 2.061(4) Å for Zn4–O2), matching observations in the literature [25, 34]. The apical water molecules show Zn–O bond lengths of 2.049(4) and 2.022(5) Å to Zn1 and Zn4, which agrees with the values reported in the literature [35]. An asymmetry is noted in the μ^3-OH–Zn distances (2.024(4) Å for Zn4–O4 to 2.083(4) Å for Zn2–O3), which is supported by the literature reports [33]. For both molecular units, the Zn–N_{imino} bonds are significantly shorter (2.037(5) for Zn2–N6, e.g.) than the metal–pyridyl nitrogen (e.g., 2.079(5) for Zn4–N8), which is confirmed by comparing with the related systems in the literature [34, 36].

3.3. *Phosphodiester hydrolysis activity*

Complexes **1**–**3** were explored as catalysts for hydrolysis reaction of the diphosphate ester BNPP. The BNPP is a common model substrate because hydrolysis leads to the formation of *p*-nitrophenolate, which can be easily monitored spectroscopically by the strong absorbance at 414 nm. The hydrolysis of phosphate esters is known to be pH

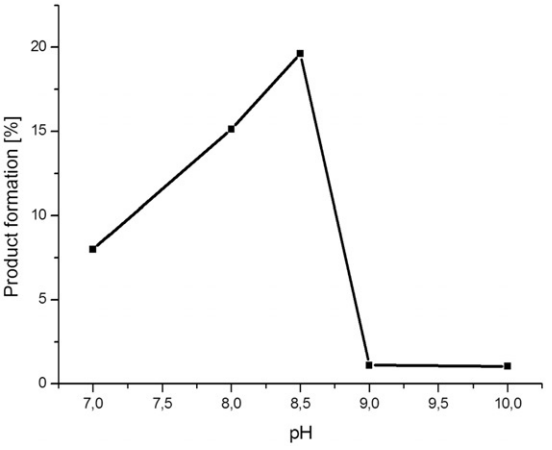

Figure 3. Effect of pH on BNPP hydrolysis mediated by **3**. Conditions: $[\mathbf{3}]_0 = 0.4\,\mathrm{m\,mol\,L^{-1}}$, $[\mathrm{BNPP}]_0 = 0.8\,\mathrm{m\,mol\,L^{-1}}$ at 50°C in a buffered mixture of H_2O and DMSO (1 : 6).

dependant [9, 10]. For this reason, we investigated the hydrolysis reaction in buffered water/DMSO solutions between pH 7 and 10 at 50°C. The poor solubility of the complexes in aqueous solutions required the use of a solvent mixture of water and DMSO in a 1 : 6 ratio. The optimal operating conditions found a distinct maximum activity at pH 8.5 for **3**, as derived from the activity profile depicted in figure 3. It also shows that the compound decomposes in more basic media.

At the optimal pH of 8.5 (buffered with *N*-tris(hydroxymethyl)methyl–3-aminopropanesulfonic acid, TAPS, in H_2O/DMSO = 1 : 6), hydrolysis of BNPP catalyzed by **1**–**3** was followed by UV-Vis spectroscopy. Control experiments with zinc perchlorate, zinc chloride, or in the absence of a zinc salt did not show any product formation under these conditions. The results of catalytic product formation after 25, 100, and 200 min are summarized in table 3. The chloro complex (**3**) was most active, whereas the hydroxyl-bridged **1** showed poor activity.

Kinetic data were obtained from the UV-Vis experiments. The absorbance of the formed product at 414 nm was corrected for catalyst absorption. k_{obs} and v_0 for the three compounds were obtained by employing the following equations:

$$y = A_1 - A_2 \cdot e^{-k_{obs} \cdot x}$$
$$y'(0) = A_2 \cdot k_{obs} = v_0$$

A comparison of the obtained k_{obs} in $[1\,s^{-1}]$ $(1.10(1) \cdot 10^{-4}$ for **1**, $2.70(1) \cdot 10^{-4}$ for **2**, and $2.70(6) \cdot 10^{-4}$ for **3**), and v_0 $(1.54(2) \cdot 10^{-8}$ for **1**, $1.242(5) \cdot 10^{-7}$ for **2** and $1.62(4) \cdot 10^{-7}$ for **3** in $[\mathrm{mol}\,(l \cdot s)^{-1}]$) is shown in figure 4. The hydrolytic activity of **1** is lower compared to **2** and **3**, which exhibit similar k_{obs} values. The initial rates v_0 increase follows the order **1** < **2** < **3**.

The dependence of the initial rate of hydrolysis on substrate concentration was tested for **1** and **3**, the slowest and the fastest derivatives. The curves obtained by UV-Vis spectroscopy were fitted by applying the aforementioned exponential rate law. The initial rates were linearly dependent on the concentration of substrate at very low

Table 3. *p*-Nitrophenolate formation mediated by **1**–**3**.

	25 min[a]	100 min[a]	200 min[a]
$Zn(ClO_4)_2$ or no catalyst	0	0	0
$[\{Zn_2L(\mu^3\text{-}OH)(H_2O)\}_2](ClO_4)_4$ (**1**)	4	9	14
$[Zn_2L(CH_3COO)_3]$ (**2**)	22	47	58
$[Zn_2LCl_3]$ (**3**)	37	68	81

Conditions: $2[\mathbf{1}]_0 = [\mathbf{2}]_0 = [\mathbf{3}]_0 = 0.4\,\text{mmol L}^{-1}$, $[\text{BNPP}]_0 = 0.8\,\text{mmol L}^{-1}$ at 50°C, pH 8.5 in buffered H_2O/DMSO 1 : 6.
[a]In % *p*-nitrophenolate formed.

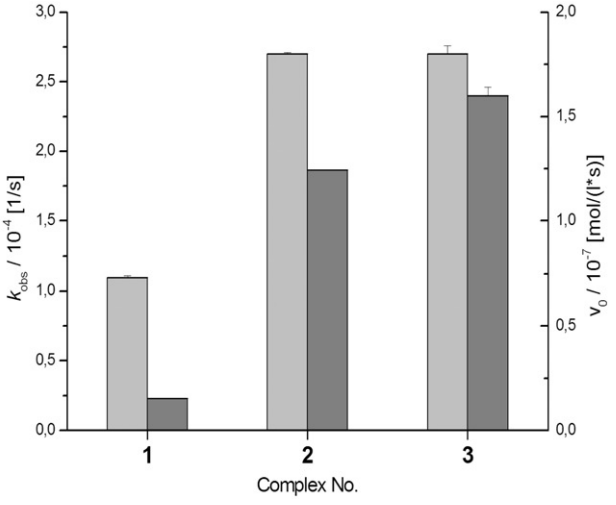

Figure 4. Rate constants k_{obs} (light grey, left) and initial rates v_0 (dark grey, right) for **1**–**3**.

excesses of the latter. For higher substrate concentrations a decreased reaction rate was observed, which can be explained by a complex-substrate pre-equilibrium. Such behavior is generally known for native enzymes and can be fitted to a standard Michaelis–Menten rate law. Fitting of the data (figure 5) yielded values for K_M and v_{max}. To evaluate the catalytic efficiency of the present system to existing catalysts, the specifity constant k_2 ($=k_{cat}/K_M$) is calculated, as this value can directly be compared to the rate constant k_2 of simple second-order processes.

Table 4 shows that **1** and **3** show higher activities than those of comparable systems with larger metal–metal distances. The obtained data are similar to many unsymmetric or heterobimetallic systems [21]. The exact mechanism of the nucleophilic attack on the phosphorus center is still under debate. There exist three main proposals on how nucleophilic attack of the substrate by a hydroxide can occur: (a) by the bridging OH between two Zn centers; (b) by a terminal OH at one Zn; or (c) by an activated H_2O in the vicinity of the active site [4, 5]. Compound **1** with a bridging OH and thus a relatively short Zn–Zn distance shows the lowest hydrolytic activity arguing against a mechanism according to (a) in the present system. In addition, we have no evidence for a bridging OH group in **2** and **3**. For these reasons, we believe that in this system a

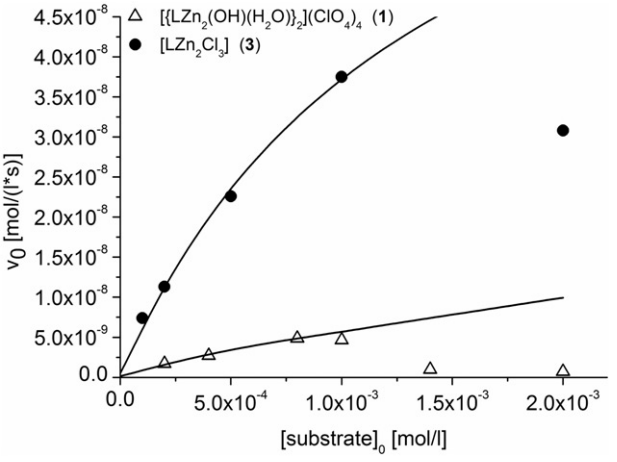

Figure 5. Dependence of the initial rate of BNPP hydrolysis mediated by **1** and **3** on substrate concentration. Conditions: $2[\mathbf{1}]_0 = [\mathbf{3}]_0 = 0.1\,\mathrm{m\,mol\,L^{-1}}$, 50°C, pH 8.5, buffered water/DMSO 1 : 6.

Table 4. Kinetic data for BNPP hydrolysis promoted by **1** and **3**.

	$[\{Zn_2L(\mu^3\text{-}OH)(H_2O)\}_2](ClO_4)_4$ (**1**)	$[Zn_2LCl_3]$ (**3**)
K_M[a]	$1.84(0.89)\cdot 10^{-2}$	$1.38(0.38)\cdot 10^{-2}$
v_{max}[b]	$1.60(0.5)\cdot 10^{-8}$	$8.86(1.6)\cdot 10^{-8}$
k_{cat}[c]	$1.60\cdot 10^{-4}$	$8.86\cdot 10^{-4}$
k_2[d]	$0.87\cdot 10^{-1}$	$6.40\cdot 10^{-1}$

Conditions: $2[\mathbf{1}]_0 = [\mathbf{3}]_0 = 0.1\,\mathrm{mmol\,L^{-1}}$, 50°C, pH 8.5, buffered water/DMSO = 1 : 6.
[a]In $\mathrm{mol\,L^{-1}}$; [b]in $\mathrm{mol\,(L\cdot s)^{-1}}$; [c]in $1\,\mathrm{s^{-1}}$; [d]in $\mathrm{L\,(mol\cdot s)^{-1}}$.

terminal hydroxide nucleophile is involved as shown by the presence of a coordinated water in the crystal structure of **1**. However, since all reactions were performed in a solvent mixture with a high content of DMSO, alteration of the reactivity due to solvent coordination cannot be ruled out. We believe that the higher rate of catalysis observed with chloro compound (**3**) is due to its higher electrophilic nature in comparison to the perchlorate derivative (**1**). This electronic influence is particularly pronounced in these compounds featuring a ligand with low denticity since in this case substrate and nucleophile can easily access the active site. Allosteric substrate inhibition is observed as a drawback, presumably from the opposite side of the planar complex.

4. Conclusions

The reaction of a tridentate bis(pyridylmethyl) phenolate with three zinc salts led to the formation of three complexes with two zinc ions in the ligand scaffold. X-ray crystallography of a single crystal of **1** revealed a tetranuclear structure with an open Zn_4O_4 hetero-cubane core featuring two μ^3-OH moieties. The compounds were

catalysts for hydrolysis of BNPP. Kinetic investigations showed **3** to be the most active and **1** with a bridging OH to be the least active. Thus, in this system a mechanism *via* a bridging OH seem not to be a requirement, and we attribute the higher activity of **3** to the more electrophilic nature of Zn.

Supplementary material

Crystallographic data (without structure factors) for **1** have been deposited with the Cambridge Crystallographic Data Centre (CCDC) as supplementary publication no. CCDC-818714. Copies of the data can be obtained free of charge from the CCDC (12 Union Road, Cambridge CB2 1EZ, UK; Tel.: +44-1223-336408; Fax: +44-1223-336003; Email: deposit@ccdc.cam.ac.uk; Website: http:/www.ccdc.cam.ac.uk).

Acknowledgments

The authors acknowledge FForte – Wissenschafterinnenkolleg FreChe Materie for financial support.

References

[1] J. Weston. *Chem. Rev.*, **105**, 2151 (2005).
[2] N. Sträter, W.N. Lipscomb, T. Klabunde, B. Krebs. *Angew. Chem. Int. Ed.*, **35**, 2024 (1996).
[3] D.E. Wilcox. *Chem. Rev.*, **96**, 2435 (1996).
[4] M. Jarenmark, E. Csapo, J. Singh, S. Wöckel, E. Farkas, F. Meyer, M. Haukka, E. Nordlander. *Dalton Trans.*, 8183 (2010).
[5] E. Kimura. *Curr. Opin. Chem. Biol.*, **4**, 207 (2000).
[6] J. Chin. *Curr. Opin. Chem. Biol.*, **1**, 514 (1997).
[7] F. Mancin, P. Tecilla. *New J. Chem.*, **31**, 800 (2007).
[8] W.H. Chapman Jr, R. Breslow. *J. Am. Chem. Soc.*, **117**, 5462 (1995).
[9] B. Bauer-Siebenlist, F. Meyer, E. Farkas, D. Vidovic, J.A. Cuesta-Seijo, R. Herbst-Irmer, H. Pritzkow. *Inorg. Chem.*, **43**, 4189 (2004).
[10] B. Bauer-Siebenlist, F. Meyer, E. Farkas, D. Vidovic, S. Dechert. *Chem. Eur. J.*, **11**, 4349 (2005).
[11] G. Feng, J.C. Mareque-Rivas, R.T. de Martin Rosales, N.H. Williams. *J. Am. Chem. Soc.*, **127**, 13470 (2005).
[12] G. Feng, J.C. Mareque-Rivas, N.H. Williams. *Chem. Commun.*, 1845 (2006).
[13] G. Feng, D. Natale, R. Prabaharan, J.C. Mareque-Rivas, N.H. Williams. *Angew. Chem. Int. Ed.*, **45**, 7056 (2006).
[14] M.F. Mohamed, A.A. Neverov, R.S. Brown. *Inorg. Chem.*, **48**, 11425 (2009).
[15] A. Neves, M. Lanznaster, A.J. Bortoluzzi, R.A. Peralta, A. Casellato, E.E. Castellano, P. Herrald, M.J. Riley, G. Schenk. *J. Am. Chem. Soc.*, **129**, 7486 (2007).
[16] H. Adams, L.R. Cummings, D.E. Fenton, P.E. McHugh. *Inorg. Chem. Commun.*, **6**, 19 (2003).
[17] H. Adams, D. Bradshaw, D.E. Fenton. *Dalton Trans.*, 3407 (2001).
[18] M. Jarenmark, S. Kappen, M. Haukka, E. Nordlander. *Dalton Trans.*, 993 (2008).
[19] A. Roth, E.T. Spielberg, W. Plass. *Inorg. Chem.*, **46**, 4362 (2007).
[20] A. Roth, A. Buchholz, M. Rudolph, E. Schütze, E. Kothe, W. Plass. *Chem. Eur. J.*, **14**, 1571 (2008).
[21] L.R. Gahan, S.J. Smith, A. Neves, G. Schenk. *Eur. J. Inorg. Chem.*, 2745 (2009).
[22] K. Shanmuga Bharathi, S. Sreedaran, A. Kalilur Rahiman, K. Rajesh, V. Narayanan. *Polyhedron*, **26**, 3993 (2007).
[23] N.A. Rey, A. Neves, A.J. Bortoluzzi, C.T. Pich, H. Terenzi. *Inorg. Chem.*, **46**, 348 (2007).

[24] Y.D.M. Champouret, W.J. Nodes, J.A. Scrimshire, K. Singh, G.A. Solan, I. Young. *Dalton Trans*., 5465 (2007).
[25] K. Selmeczi, C. Michel, A. Milet, I. Gaultier-Luneau, C. Philouze, J.L. Pierre, D. Schnieders, A. Rompel, C. Belle. *Chem. Eur. J*., **13**, 9093 (2007).
[26] K. Abe, J. Izumi, M. Ohba, T. Yokoyama, H. Okawa. *Bull. Chem. Soc. Jpn*., **74**, 85 (2001).
[27] R.R. Gagne, R.P. Kreh, J.A. Dodge. *J. Am. Chem. Soc*., **101**, 6917 (1979).
[28] C.J. O'Connor, D. Firmin, A.K. Pant, B.R. Babu, E.D. Stevens. *Inorg. Chem*., **25**, 2300 (1986).
[29] T. Mallah, O. Kahn, J. Gouteron, S. Jeannin, Y. Jeannin, C.J. O'Connor. *Inorg. Chem*., **26**, 1375 (1987).
[30] T. Ichinose, Y. Nishida, H. Okawa, S. Kida. *Bull. Chem. Soc. Jpn*., **47**, 3045 (1974).
[31] J. Hermann, A. Erxleben. *Inorg. Chim. Acta*, **304**, 125 (2000).
[32] A.W. Addison, T.N. Rao, J. Reedijk, J. van Rijn, G.C. Verschoor. *Inorg. Chem*., **23**, 1349 (1984).
[33] G. Marinescu, G. Marin, A.M. Madalan, A. Vezeanu, C. Tiseanu, M. Andruh. *Cryst. Growth Des*., **10**, 2096 (2010).
[34] W. Huang, S. Gou, H. Qian, D. Hu, S. Chantrapromma, H.K. Fun, Q. Meng. *Eur. J. Inorg. Chem*., 947 (2003).
[35] G.S. Papaefstathiou, I.G. Georgiev, T. Friscic, L.R. MacGillivray. *Chem. Commun*., 3974 (2005).
[36] Bruker AXS Inc., *SADABS V2008-1*, Bruker, Madison, WI, USA (2008).